

Magnetorotational explosions of core-collapse supernovae

G.S.Bisnovaty-Kogan¹, S.G.Moiseenko², N.V.Ardeljan³

¹*Space Research Institute, Profsoyuznaya str. 84/32, Moscow 117997, Russia, and National Research Nuclear University "MEPHI", Kashirskoye Shosse, 31, Moscow 115409, Russia*

²*Space Research Institute, Profsoyuznaya str. 84/32, Moscow 117997, Russia*

³*Department of Computational Mathematics and Cybernetics, Moscow State University, Vorobjevy Gory, Moscow B-234, Russia*

Corresponding author: gkogan@iki.rssi.ru

Abstract

Core-collapse supernovae are accompanied by formation of neutron stars. The gravitation energy is transformed into the energy of the explosion, observed as SN II, SN Ib,c type supernovae. We present results of 2-D MHD simulations, where the source of energy is rotation, and magnetic field serves as a "transition belt" for the transformation of the rotation energy into the energy of the explosion. The toroidal part of the magnetic energy initially grows linearly with time due to differential rotation. When the twisted toroidal component strongly exceeds the poloidal field, magneto-rotational instability develops, leading to a drastic acceleration in the growth of magnetic energy. Finally, a fast MHD shock is formed, producing a supernova explosion. Mildly collimated jet is produced for dipole-like type of the initial field. At very high initial magnetic field no MRI development was found.

Keywords: Core-collapse supernova - Magnetorotational mechanism - Numerical modeling.

1 Introduction

Supernova is one of the most powerful explosion in the Universe which releases about 10^{51} erg both in radiation and kinetic energies. SNe explode at the end of evolution of massive stars, with initial mass larger than $\sim 8M_{\odot}$. A thermonuclear explosion of C-O degenerate core with total disruption of the star takes place in SN Ia, what happens when initial mass of the star does not exceed $\sim 12M_{\odot}$, when the electrons are degenerate in the carbon-oxygen core. For larger initial masses the evolution proceeds until the formation of the iron core, and the star collapses due to a loss of a hydrodynamic stability. During the core collapse and formation of a neutron star, gravitational energy release $\sim 6 \cdot 10^{53}$ erg, is carried away by neutrino. The first mechanism suggested in [15] for the explanation of the explosion in a core-collapse SN was connected with a neutrino deposition. The huge energy flux carried by neutrino heats the infalling outer layers, reverse the direction of motion, and leads to formation of the shock wave, producing explosions of SN II, SN Ib,c types. Later more accurate calculations revealed that the energy of such explosion is not enough for the explanation of observations. Many modifications of the neutrino model have been calculated during years, but the problem is not yet clear. The review of the problem may be found in the book [8].

In recent simulations (see details in [23]) we have found that for extremely strong initial magnetic field $H_0 = 10^{12}$ G a prompt supernova explosion occurs, and collimated jet is formed in agreement with [28]. For case when the initial magnetic field is weaker $H_0 = 10^9$ G we have identified, after the linear growth of the poloidal magnetic field due to differential rotation, the exponential field growth due to the magnetorotational instability of Tayler type [30]. We call the combination of differential rotation with the Tayler type MRI instability, as magneto-differential-rotation instability (MDRI). The ejection due to the explosion is only weakly collimated, while [28] had obtained a strong collimation in this variant also. In these simulations we considered a uniform magnetic field along the rotational axis, as the initial field configuration, similar to [28].

2 Magnetorotational mechanism of explosion

In magnetorotational explosion (MRE) the transformation of the rotational energy of the neutron star into explosion energy takes place by means of the magnetic field [7]). Neutron stars are rotating, and have magnetic fields up to 10^{13} Gs, and even more. Often one or two-side ejections are visible. That indicate to non-spherical form of the SNe explosions.

In differentially rotating new born neutron stars radial magnetic field is twisted, and magnetic pressure becomes very high, producing MHD shock by which the rotational energy is transformed to the explosion energy.

Calculations of MRE have been done in [12], using one-dimensional nonstationary equations of magnetic hydrodynamics, for the case of cylindrical symmetry. The energy source is supposed to be the rotational energy of the system (the neutron star, and surrounding envelope). The calculations show that the envelope splits up during the dynamical evolution of the system, the main part of the envelope joins the neutron star and becomes uniformly rotating with it, and the outer part of the envelope expands with large velocity, carrying out a considerable part of rotational energy and rotational momentum. MRE has an efficiency about 10% of the rotational energy, the ejected mass is ≈ 0.1 of the star mass, explosion energy $\approx 10^{51}$ erg. Ejected mass and explosion energy depend weakly on the parameter $\alpha = E_{mag}/E_{grav}$ at initial moment. Explosion time depends on α as $t_{expl} \sim \frac{1}{\sqrt{\alpha}}$. Small α is difficult for numerical calculations with explicit numerical schemes because of the Courant restriction on the time step, hard system of equations, where α determines a hardness.

3 2-D calculations

The numerical method used in simulations is based on the implicit operator-difference, completely conservative scheme on a Lagrangian triangular grid of variable structure, with grid reconstruction (Fig.1). The implicitness of the applied numerical scheme allows for large time-steps. It is important to use the implicit scheme in the presence of two strongly different time-scales: the small one due to huge sound velocity in the central parts of the star, and the big one determining the evolution of the magnetic field. The method applied here was developed and its stability was investigated in the papers of [5], [6], [1]. The scheme is fully conservative, what includes conservation of mass, momentum and total energy, and correct transitions between different types of energies. It was tested thoroughly with different tests by [2].

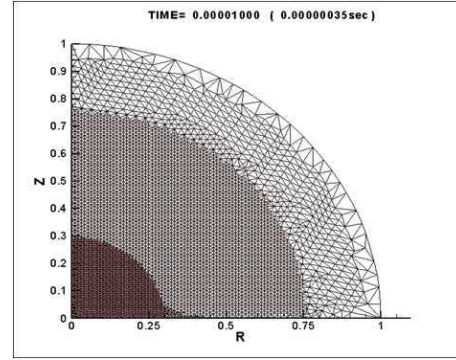


Figure 1: Example of the triangular grid

In the calculations of magnetorotational core-collapse supernova performed by [3], magnetohydrodynamic (MHD) equations with self-gravitation, and infinite conductivity have been solved using the numerical scheme as described above. The problem has an axial symmetry ($\frac{\partial}{\partial \phi} = 0$), and the symmetry to the equatorial plane ($z=0$). Initial toroidal current J_ϕ was taken at the initial moment (time started now from the stationary rotating neutron star) producing H_r , H_z according to Biot-Savart law $\mathbf{B} = \frac{1}{c} \int_V \frac{\mathbf{J} \times \mathbf{R}}{R^3} dV$. Initial magnetic field of quadrupole-like symmetry is obtained at opposite directions of the current in both hemispheres. Neutrino cooling was calculated using a variant of a flux-limited method, [3].

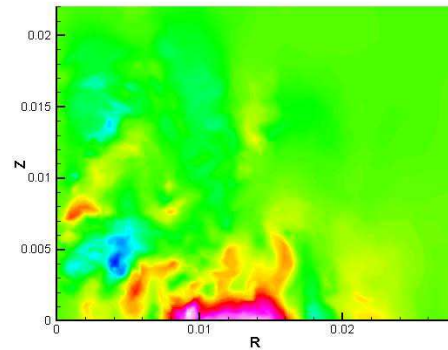


Figure 2: Toroidal magnetic field distribution at the moment of its maximal energy for the initial quadrupole field.

Magnetic field is amplified due to twisting by the differential rotation, and subsequent development of the magnetorotational instability. The field distribution for initial quadrupole-like magnetic field with $\alpha = 10^{-6}$, at the moment of the maximal energy of the toroidal magnetic field is represented in Fig.1. The maximal value of $B_\phi = 2.5 \cdot 10^{16}$ Gs was obtained in the calculations. The magnetic field at the surface of the neutron star after the explosion is $B = 4 \cdot 10^{12}$ Gs. Time dependence during the explosion of rotational, gravitational, internal, and kinetic poloidal

energies is given in Figs.3. Almost all gravitational energy, transforming into heat during the collapse, is carried away by weakly interacting neutrino. The total energy ejected in the kinetic form is $\sim 0.6 \cdot 10^{51}$ erg, and the total ejected mass is equal to $\sim 0.14 M_{\odot}$.

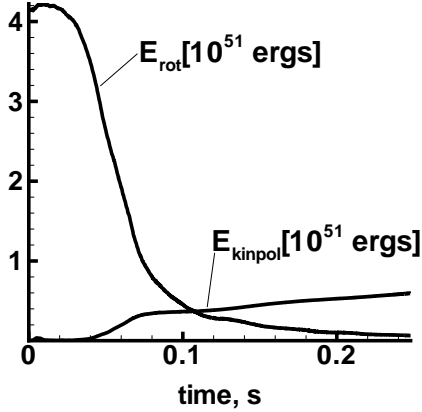


Figure 3: Time dependence of rotational, kinetic poloidal, and magnetic energies during explosion for a dipole-like field, from [22].

The simulations were done for the initial poloidal magnetic field of quadrupole [3] and of dipole [22] types of symmetry. Before the collapse the ratios between the rotational and gravitational, and between the internal and gravitational energies of the star had been chosen as: $\frac{E_{rot}}{E_{grav}} = 0.0057$, $\frac{E_{int}}{E_{grav}} = 0.727$. The initial magnetic field was "turned on" after the collapse stage. The ratio between the initial magnetic and gravitational energies was chosen as 10^{-6} . The initial poloidal magnetic field in the center, at start of the evolution of the toroidal field was $\sim 3.2 \times 10^{13}$ G.

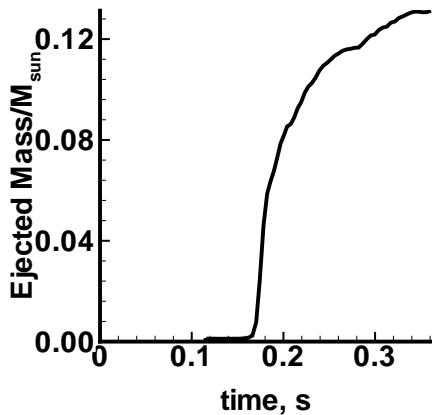


Figure 4: Time dependence of the ejected mass during the magnetorotational explosion with initial dipole magnetic field, from [22].

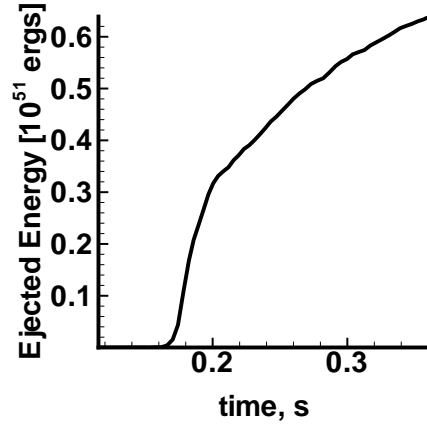


Figure 5: Time dependence of the ejected energy during the magnetorotational explosion with initial dipole magnetic field, from [22].

The magnetic field works as a piston for the originated MHD shock. The time dependence of the ejected mass and energy is given in Figs. 4, 5. During the magnetorotational explosion $\sim 0.14 M_{\odot}$ of the mass and $\sim 0.6 \cdot 10^{51}$ ergs ($\sim 10\%$ of the rotational energy) are ejected. The simulation of the MR supernova explosion for various initial core masses and rotational energies was done by [11]. The initial core mass was varied from $1.2 M_{\odot}$ to $1.7 M_{\odot}$, the initial specific rotational energy E_{rot}/M_{core} , was varied from 0.19×10^{19} to 0.4×10^{19} erg/g. The explosive energy increases with the mass of the core, and the initial rotational energy. The energy released in MR explosion, $(0.5 - 2.6) \times 10^{51}$ erg, is sufficient to explain supernova with collapsing cores, Types II and Ib. The energies of Type Ic supernovae could be higher.

4 Magnetorotational instability

Magnetorotational instability (MRI) leads to exponential growth of magnetic fields. Different types of MRI have been studied by [31], [27]. MRI starts to develop when the ratio of the toroidal to poloidal magnetic energies is becoming large. In 1-D calculations MRI is absent because of a restricted degree of freedom, and time of MR explosion is increasing with α as $t_{expl} \sim \frac{1}{\sqrt{\alpha}}$, $\alpha = \frac{E_{mag0}}{E_{grav0}}$. Due to development of MRI the time of MR explosion depends on α much weaker. The MR explosion happens when the magnetic energy is becoming comparable to the internal energy, at least in some parts of the star. While the starting magnetic energy linearly depends on α , and MRI leads to exponential growth of the magnetic energy, the total time of MRE in 2-D is growing **log-**

arithmically with decreasing of α , $t_{expl} \sim -\log \alpha$. These dependencies are seen clearly from 1-D ([12]) and 2-D calculations ([3], [22]) giving the following explosion times t_{expl} (in arbitrary units): $\alpha = 0.01$, $t_{expl} = 10$, $\alpha = 10^{-12}$, $t_{expl} = 10^6$ in 1-D, and $\alpha = 10^{-6}$, $t_{expl} \sim 6$, $\alpha = 10^{-12}$, $t_{expl} \sim 12$ in 2-D. The dependence of the explosion time is shown in graphs for the quadrupole ([21]), and dipole ([22]) configurations of the magnetic field. The qualitative picture of the MRI in 2D, and the example of the analytical toy model with an exponential growth of the magnetic field, have been presented by [3], [22].

5 Jet formation in MRE

Jet formation in MRE happens when the initial magnetic field is of a dipole structure. 2-D calculations with the initial dipole-like magnetic field gave almost the same values of the energy of explosion $\sim 0.5 \cdot 10^{51}$, and ejected mass $\approx 0.14M_{\odot}$, but the outburst was slightly collimated along the rotational axis [22], see Figs.6,7

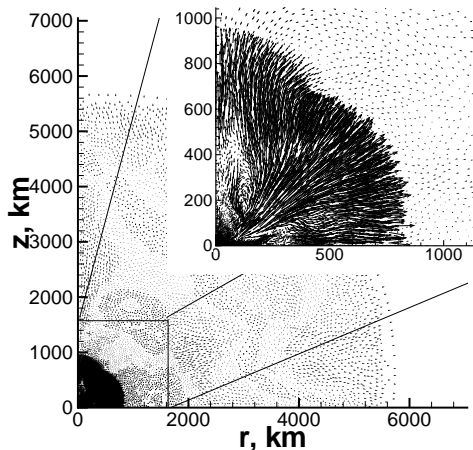


Figure 6: Time evolution of the velocity field (out-flow) for the time moment $t = 0.075s$, from [22]

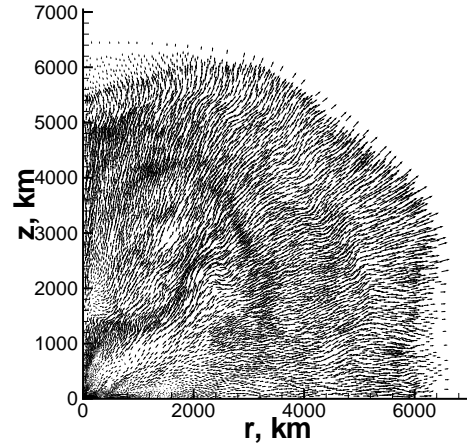


Figure 7: Time evolution of the velocity field (out-flow) for the time moment, $t = 0.25s$, from [22].

Simulations of the MR supernova have been made with equation of state suggested in [25]. A comparison of our results for the initially uniform magnetic field, using a Lagrangian scheme, with the results in [28] and [29], using an Eulerian scheme for the same initial and boundary conditions, shows good agreement for a strong initial field ($H_0 = 10^{12}G$), while for a weaker field ($H_0 = 10^9G$) we get mildly collimated jet-like explosion; see also [13]. Details of the results of these simulations will be published elsewhere ([23]). MRI is developed in the case of a weaker initial magnetic field, and it is not present in the calculations with stronger field, see Figs.8,12.

We have made simulations for the initial magnetic fields $H_0 = 10^9, 10^{12}G$. The ratio of the initial rotational energy to the absolute value of the gravitational energy was taken $E_{rot0}/E_{grav0} = 1\%, 2\%$. When the initial magnetic field is moderate ($H_0 = 10^9G$) and $E_{rot0}/E_{grav0} = 1\%$ MDRI develops what means exponential growth of all components of the magnetic field (Fig.8).

At Fig.9 The Lagrangian triangular grid and the ratio of the toroidal magnetic energy to the poloidal one (E_{tor}/E_{pol}) is represented for the case $H_0 = 10^9G$, and $E_{rot0}/E_{grav0} = 1\%$. The toroidal magnetic energy dominates over the poloidal one in the significant part of the region where new neutron star is forming. The MDRI is well-resolved on our triangular grid.

In the case ($H_0 = 10^{12}G$) and $E_{rot0}/E_{grav0} = 1\%$ there is no regions of domination of E_{tor} over E_{pol} .

The Fig.10 represents a time evolution of rotational, magnetic poloidal and toroidal energies for MR explosion when $H_0 = 10^9G$.

The Fig.11 is the same data plot as the Fig.10 but zoomed and the vertical axis is in logarithmic scale. The straight dash-dotted line at the Fig.11 shows the exponential growth of the toroidal and poloidal mag-

netic energies with the time due to the MDRI.

The rotational energy has two maxima. The first contraction is accompanied by the strong growth of the rotational energy due to angular momentum conservation, maximum of which coincides with the first maximum of the density. The first contraction, and the subsequent bounce, happens when the magnetic field is growing slowly, and the angular momentum losses from the stellar core are small. Development of the magnetorotational instability leads to a rapid growth of the magnetic field, large angular momentum flux from the core, what stops the expansion, and leads to the second contraction phase. In this case the contraction is not transforms into expansion, because of the rapid decrease of the rotational energy due to strong angular momentum flux outside from the core.

The energy of the poloidal magnetic field grows due to the contraction until the time $t \approx 0.225$ sec. Then it slightly decreases because of the formation of the bounce shock, and its motion outwards. The toroidal magnetic energy grows as quadratic function because of wrapping of the magnetic force lines (toroidal component of the magnetic field grows linearly). Starting from $t \approx 0.3$ sec both the poloidal and toroidal magnetic energies begin to grow exponentially due to MDRI. At $t \approx 0.36$ sec both magnetic energies comes to saturation. The MHD shock wave develops what leads to the MR explosion. The MR explosion develops in all directions without formation of a collimated flow.

The MR explosion for an extremely high initial magnetic field ($H_0 = 10^{12}$ G) is developing in a qualitatively different way. The initial magnetic field is so strong that it grows strongly during the first contraction, and the explosion happens before the development of MDRI happens (Fig.12). At the Fig.13 the time evolution of the rotational, poloidal magnetic and toroidal magnetic energies are represented. The rotational energy has one extremum at $t \approx 0.32$ sec corresponds to the maximal contraction, accompanied by a corresponding growth of of the toroidal and poloidal magnetic energies. The poloidal magnetic field grows due to the contraction, the toroidal magnetic field appears due to the differential rotation and is amplified both due to the differential rotation and the contraction of the core.

The strong initial magnetic field leads to a rapid loss of the angular momentum from the core already during the contraction phase. The centrifugal force becomes unimportant, and the first contraction is not followed by any bounce, leaving behind a dense slowly rotating neutron star core. We have got here a prompt explosion.

The force lines of the magnetic field play the role of 'rails'. The matter moves along the force lines. The magnetic pressure dominates a the periphery of

the core. The MR explosion develops mainly along the axis of rotation, and the collimated flow (protojet) is formed. The MR explosion results in the collimated jet. The degree of jet collimation is approximately the same as in [28]. For the case when $E_{rot0}/E_{grav0} = 1\%$ and $H_0 = 10^9$ G the MR supernova explosion energy is $\sim 4 \times 10^{50}$ erg, for the $H_0 = 10^{12}$ G the MR supernova explosion energy reaches the value of $\sim 8 \times 10^{50}$ erg. The explosion energy resulted in the simulations by Lagrangian method are close to those ones found in the simulations made by Eulerian scheme [28] (excluding the case of $B_0 = 10^{12}$ G and $E_{rot0}/|E_{grav0}| = 1/\%$).

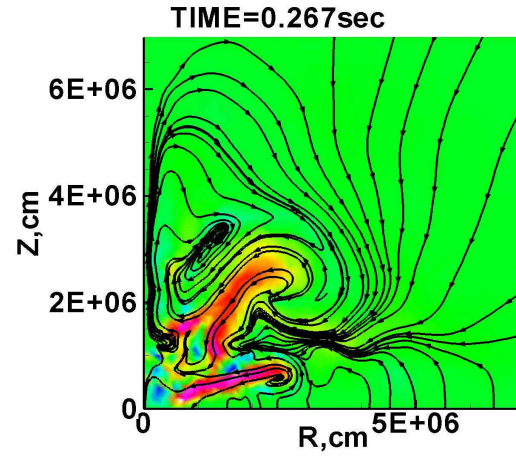


Figure 8: Developed MDRI due to convection and MRI/Taylor instability at $t = 267$ ms for the case $H_0 = 10^9$ G, $E_{rot0}/E_{grav0} = 1\%$ (contour plot - the toroidal magnetic field, arrow lines - force lines of the poloidal magnetic field).

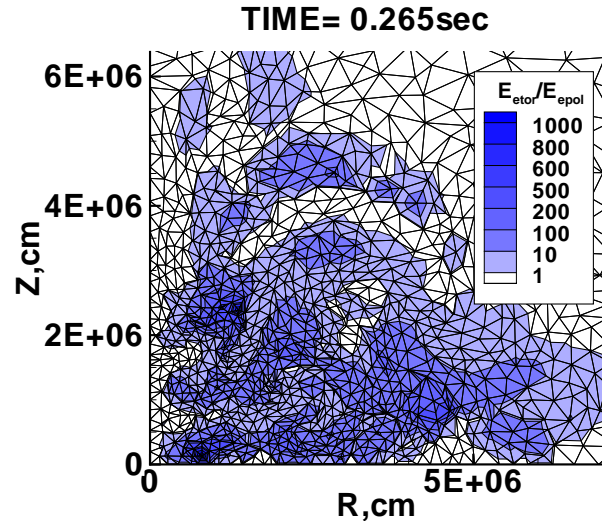


Figure 9: The Lagrangian triangular grid and the ratio of the toroidal magnetic energy E_{tor} to the

poloidal magnetic energy E_{pol} , $\frac{E_{tor}}{E_{pol}}$ at $t = 265\text{ms}$ for the case $H_0 = 10^9\text{G}$, $E_{rot0}/E_{grav0} = 1\%$.

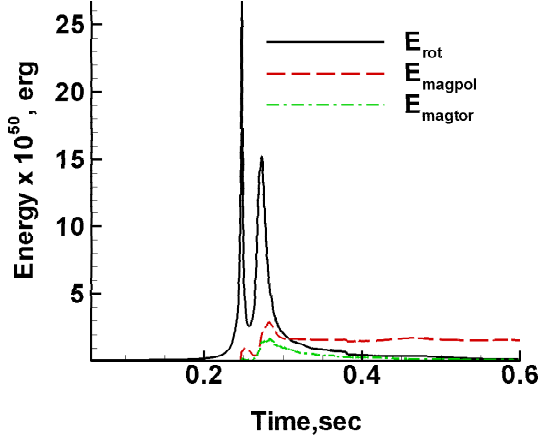


Figure 10: Time evolution of rotational energy E_{rot} (solid line), magnetic poloidal energy E_{magpol} (dashed line) and magnetic toroidal energy E_{magtor} (dash-dotted line) for the case $H_0 = 10^9\text{G}$, $E_{rot0}/E_{grav0} = 1\%$.

6 Asymmetry of the explosion

It is known from the observations that the shapes of core collapse supernovae are different. From our simulations it follows that MR supernova explosion arises after development of the MRI. The development of the MRI is a stochastic process and hence the resulting shape of the supernova can vary. We may conclude that MR supernova explosion mechanism can lead to different shape of the supernova. It is important to point out that MR mechanism of supernova explosion leads always to asymmetrical outbursts.

The simulations of the MR supernova explosions described here are restricted by the symmetry to the equatorial plane. While in reality this symmetry can be violated due to the MRI, simultaneous presence of the initial dipole and quadrupole -like magnetic field ([33]) and initial toroidal magnetic field ([10]). The violation of the symmetry could lead to the kick effect and formation of rapidly moving radio pulsars. A kick velocity, along the rotational axis, formed due to magnetohydrodynamic processes in presence of the asymmetry of the magnetic field, by estimations [9] does not exceed 300km/sec.

When rotational and magnetic axes do not coincide the whole picture of the explosion process is three dimensional. Nevertheless, the magnetic field twisting happens always around the rotational axis, so we may expect the kick velocity of the neutron star

be strongly correlated with its spin direction. During the phase of MRE explosion the regular component of magnetic field may exceed temporally 10^{16}G [3], [22], when the neutrino cross-section depends on the magnetic field strength. The level of the anisotropy of the magnetic field relative to the plain perpendicular to the rotational axis [20] may be of the order of 50%, leading to strong anisotropy of the neutrino flux. The kick velocity due to the anisotropy of the neutrino flux may reach several thousands km/c [9], explaining appearance of the most rapidly moving radio pulsars [32]. Simultaneously, because of the stochastic nature of MRI, the level of the anisotropy should be strongly variable, leading to a large spreading in the the neutron star velocities. This prediction of MR explosion differs from the models with a powerful neutrino convection, where arbitrary direction of the kick velocity is expected ([14],[17]). It was claimed in [16], that proto-neutron star (PNS) convection was found to be a secondary feature of the core-collapse phenomenon, rather than a decisive ingredient for a successful explosion.

Analysis of observations of pulsars shows that rotation and velocity vectors of pulsars are aligned, as is predicted by the MR supernova mechanism. This alignment was first found in [26], and was confirmed with reliability, increasing with time, in the papers [18],[19],[24]. The alignment of the vectors can be violated in the case when the supernova explodes in a binary system.

7 Conclusions

In MRE the efficiency of transformation of rotational energy into the energy of explosion is $\sim 10\%$. MRI strongly accelerates MRE, at lower values of the initial magnetic fields. Jet formation is possible for dipole-like topology of the field. MRE energy is not sensitive to the details of the equation of state, model of the neutrino transfer, and to the choice of the numerical scheme. The observed alignment of the rotation and velocity vectors of pulsars follows directly from the MRE supernova model.

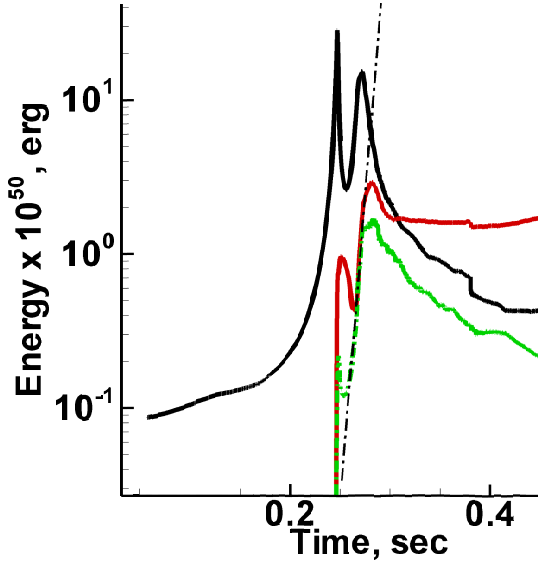


Figure 11: Zoomed time evolution of rotational energy E_{rot} (solid line), magnetic poloidal energy E_{magpol} (dashed line) and magnetic toroidal energy E_{magtor} (dash-dotted line) for the case $H_0 = 10^9 \text{G}$, $E_{rot0}/E_{grav0} = 1\%$. Straight dash-dotted line shows exponential growth of the toroidal and poloidal magnetic energies.

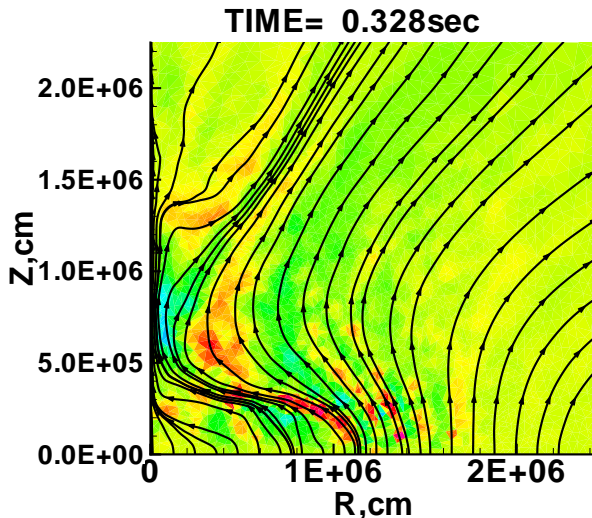


Figure 12: Absence of MDRI at $t = 328 \text{ms}$ for the case $H_0 = 10^{12} \text{G}$, $E_{rot0}/E_{grav0} = 1\%$ (contour plot - the toroidal magnetic field, arrow lines - force lines of the poloidal magnetic field).

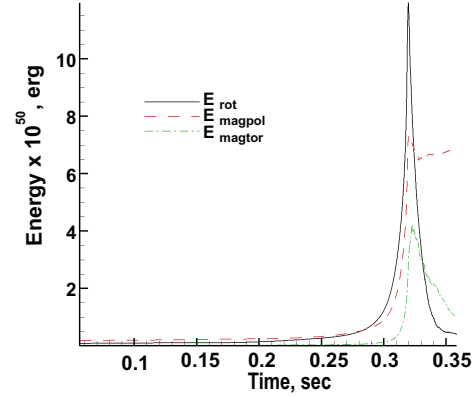


Figure 13: Time evolution of rotational energy E_{rot} (solid line), magnetic poloidal energy E_{magpol} (dashed line) and magnetic toroidal energy E_{magtor} (dash-dotted line) for the case $H_0 = 10^{12} \text{G}$, $E_{rot0}/E_{grav0} = 1\%$.

Acknowledgement

The work of SGM and GSBK was supported partially by RFBR grant 14-02-00728, grant for leading scientific schools NSH-261.2014.2, and RAS program 21/3.

References

- [1] Ardeljan, N.V., Bisnovatyi-Kogan, G.S., Kosmachevskii K.V. & Moiseenko, S.G. (1996), Astron. Ap. Suppl., 115, 573
- [2] Ardeljan, N. V., Bisnovatyi-Kogan, G. S., & Moiseenko, S. G. 2000, Astron. Ap., 355, 1181
- [3] — 2005, MNRAS, 359, 333
- [4] Ardelyan, N. V., Bisnovatyi-Kogan, G. S., & Popov, Y. P. 1979, Sov. Astron., 23, 705
- [5] Ardelyan, N.V. & Chernigovskii, S.V. 1984, Diff. Uravneniya 20, 1119.
- [6] Ardeljan, N. V., & Kosmachevskii, K. V. 1995, Comput. Math. Model., 6, 209
- [7] Bisnovatyi-Kogan, G. S. 1970, Astron. Zh., 47, 813 (SvA, 1971, 14, 652)
- [8] Bisnovatyi-Kogan, G. S. 2011, Stellar Physics 2: Stellar Evolution and Stability. Astronomy and Astrophysics Library. Springer-Verlag Berlin Heidelberg
- [9] Bisnovatyi-Kogan, G.S. 1993, Astron. Ap. Transact., 3, 287

- [10] Bisnovatyi-Kogan, G.S., Moiseenko, S.G. 1992, *Astron. Zh.*, 69, 563 (*Soviet Astronomy* 1992, 36, 285)
- [11] Bisnovatyi-Kogan, G. S., Moiseenko, S. G., & Ardelyan, N. V. 2008b, *Astronomy Reports*, 52, 997
- [12] Bisnovatyi-Kogan, G. S., Popov, I. P., & Samokhin, A. A. 1976, *Ap. Space Sci*, 41, 287
- [13] Burrows, A., Dessart, L., Livne, E., Ott, C. D. & Murphy, J. 2007, *ApJ*, 664, 416.
- [14] Burrows, A., Hayes, J., Fryxell, B.A. 1995, *ApJ*, 450, 830
- [15] Colgate, S. A. & White, R. H. 1966, *ApJ*, 143, 626
- [16] Dessart, L., Burrows, A., Livne, E., Ott, C. D. 2006, *ApJ*, 645, 534
- [17] Janka, H.-T., Müller, E. 1995, *ApJ*, 448, L109
- [18] Johnston S., Hobbs G., Vigeland S., Kramer M., Weisberg J. M., Lyne A. G., 2005, *MNRAS*, 364, 1397
- [19] Johnston, S., Kramer, M., Karastergiou, A., Hobbs, G., Ord, S., Wallman, J. 2007, *MNRAS*, 381, 1625
- [20] Mikami, H., Sato, Y., Matsumoto, T., Hanawa, T. 2008, *ApJ*, 683, 357
- [21] Moiseenko, S. G., Bisnovatyi-Kogan, G. S., & Ardeljan, N. V. 2005, *ASP Conference Series*, 342, 190. Proceedings of the conference held 15-19 June, 2004 in Padua, Italy. Edited by M. Turatto, S. Benetti, L. Zampieri, and W. Shea.
- [22] Moiseenko, S. G., Bisnovatyi-Kogan, G. S., & Ardeljan, N. V. 2006, *MNRAS*, 370, 501
- [23] Moiseenko, S. G., Bisnovatyi-Kogan, G. S., Kotake, K., Takivaki, T. & Sato, K. 2014, in preparation.
- [24] Noutsos, A., Kramer, M., Carr, P., Johnston, S. 2012, *MNRAS*, 423, 2736
- [25] Shen, H., Toki, H., Oyamatsu, K., & Sumiyoshi, K. 1998, *Nuclear Physics A*, 637, 435
- [26] Smirnova, T. V., Shishov, V. I., Malofeev, V. M. 1996, *ApJ*, 462, 289
- [27] Spruit, H.C. 2002, *Astron. Ap.*, 381, 92.
- [28] Takiwaki, T., Kotake, K., Nagataki, S., & Sato, K. 2004, *ApJ*, 616, 1086
- [29] Takiwaki, T., Kotake, K., & Sato, K. 2009, *ApJ*, 691, 1360
- [30] Tayler, R. 1973, *MNRAS*, 161, 365
- [31] Velikhov, E.P. 1959, *J. Exper. Theor. Phys.*, 36, 1398
- [32] Vlemmings, W.H.T., et al. 2005, *Mem. SAI*, 2005, 76, 531 (astro-ph/0509025)
- [33] Wang, J. C. L., Sulkanen, M. E., Lovelace, R. V. E., 1992, *ApJ*, 390, 46